Evidence for vertical phase separation in densely grafted, high-molecular-weight poly(*N*-isopropylacrylamide) brushes in water

H. Yim and M. S. Kent
Sandia National Laboratories, Department 8332, Albuquerque, New Mexico 87185, USA

S. Satija
National Institute of Standards and Technology, Gaithersburg, Maryland 20899, USA

S. Mendez, S. S. Balamurugan, S. Balamurugan, and G. P. Lopez
University of New Mexico, Albuquerque, New Mexico 87131, USA

(Received 4 May 2005; revised manuscript received 1 September 2005; published 2 November 2005)

The detailed conformational change of poly(*N*-isopropylacrylamide) (PNIPAM) brushes at high grafting density in D_2O was investigated as a function of temperature using neutron reflection. PNIPAM chains were grafted at high surface density from gold and silicon oxide surfaces by atom transfer radical polymerization. Whereas single layer profiles were observed for temperatures below and above the transition region, bilayer profiles were observed for a narrow range of temperatures near the transition. This nonmonotonic change in the concentration profile with temperature is discussed in the context of theoretical models of vertical phase separation within a brush.

DOI: 10.1103/PhysRevE.72.051801 PACS number(s): 61.25.Hq, 61.12.Ha, 61.41.+e

Water-soluble polymers have been known to exhibit unusual bulk solution behavior due to hydrogen bonding. Water-soluble polymers are important in many applications such as aqueous colloidal dispersions [1], controlled drug delivery [2], solute separation [3], tissue culture substrates [4], and controlling bioadhesion [5]. This class of polymers has been the subject of intense theoretical treatment in recent years. A number of "two state" models have been proposed in which monomers interconvert between hydrophobic and hydrophilic states. These models differ in the presumed physical origin of the two states [6–10]. For example, monomer-monomer contacts may suppress hydrogen bonding with water [6–8], or cause a difference in dipole moment due to an internal bond rotation [9]. These two state models result in an effective interaction parameter χ_{eff} that is a function of both the monomer volume fraction ϕ and the temperature T. While the two state models were originally motivated by experiments involving poly(ethylene oxide) (PEO), they may well extend to other water-soluble polymers such as (N-isopropylacrylamide) (PNIPAM). PNIPAM exhibits a lower critical solution temperature (LCST) of $\sim 30\,^{\circ}\mathrm{C}$ in water that is attributed to alterations in the hydrogen bonding interactions of the amide group [11–14].

Wagner *et al.* [15] and Mattice *et al.* [16] applied *n*-cluster theory [10] to the behavior of polymer coils and brushes. In addition to a coil-to-globule transition for dilute free chains in worse than θ conditions, they first suggested the possibility of a vertical phase separation within polymer brushes leading to a bilayer concentration profile. More recently, Baulin and Halperin studied the collapse of water-soluble polymer brushes using both a microscopic model based on the Pincus appproximation (assumes uniform stretching but allows spatial variation in segment density and in the distribution of chain ends) [17] and self-consistent field (SCF) theory [18]. The concentration profiles obtained from the two theories are very similar. They pointed out that a vertical phase separation is predicted by all two state models with suitably strong dependence $\chi_{eff}(\phi,T)$, where the free energy per lattice site is expressed as

$$f_{\infty}(\phi,T)/kT = (1-\phi)\ln(1-\phi) + \chi_{eff}(\phi,T)\phi(1-\phi).$$

This form corresponds to the $N\rightarrow\infty$ limit, where N is the degree of polymerization. For a sufficiently strong dependence $\chi_{eff}(\phi,T)$, f_{∞} exhibits a concave, unstable region in the range $\phi_{-}<\phi<\phi_{+}$ where demixing yields a concentrated inner phase at ϕ_{+} and a dilute outer phase at ϕ_{-}. For sufficiently high grafting density (σ) they showed, for the case of $\bar{\chi}=1/2+\chi_2\phi^2$ where $\bar{\chi}=\chi_{eff}-(1-\phi)\partial\chi_{eff}/\partial\phi$ and χ_2 depends on T, that with increasing χ_{eff} (or T) the segment profile changes from a dilute expanded single layer to a somewhat contracted bilayer and then to a more contracted single layer. Regarding the effect of grafting density, they distinguished two regimes. For $\sigma<\sigma_c$, where the concentration at the grafting surface ϕ_o is less than ϕ_{-}, no phase separation occurs. On the other hand, vertical phase separation occurs for higher grafting densities such that $\phi_o>\phi_{-}$. They also calculated profiles for grafted PNIPAM layers at 28 °C using experimental data for $\bar{\chi}(\phi)$ obtained from the recent study of PNIPAM phase behavior by Afroze *et al.* [19]. This analysis also resulted in bilayer profiles near the transition at high σ and single layer profiles at low σ. Thus, in addition to the effect of temperature, the variation in profile shape with grafting density is an important testable prediction of this theory. The effect of molecular weight (MW) on the concentration profile was not examined.

Regarding experimental evidence for a vertical phase transition, indirect evidence has been reported for PNIPAM and PEO brushes. Zhu and Napper [20,21] studied PNIPAM brushes grafted to polystyrene latex particles immersed in

water. The change in particle diameter was measured using dynamic light scattering as a function of temperature, showing dramatic decreases in thickness upon heating both below and above the θ temperature (30 °C). They suggested that the coil-to-globule transition at temperatures below θ was driven by relatively weak n-body interactions whereas above θ the changes in thickness were due to much stronger attractive binary interactions. This two stage collapse may suggest an interpretation in terms of a vertical phase separation [18]. More recently, Balamurugan *et al.* used surface plasmon resonance (SPR) and water contact angle measurements to characterize PNIPAM brushes grafted by atom transfer radical polymerization (ATRP) [22]. The SPR measurements indicated a gradual change in film thickness, whereas the contact angle changed abruptly at $\sim 32\,^{\circ}\mathrm{C}$. They interpreted these results in terms of a bilayer profile. They suggested that the outermost region of the brush remains highly solvated until the LCST, while the densely packed, less solvated segments within the brush undergo dehydration over a broad range of temperatures. Finally, Hu and Wu reported evidence for a clustering-induced collapse of a PEO brush [23]. The PEO chains were grafted to PNIPAM microgels. With increasing T, the portion of the hydrodynamic radius contributed by the grafted PEO (ΔR_h) initially increased as the microgel contracted and the grafting density of PEO increased. However at 32 °C, ΔR_h began to decrease sharply (a factor of 6 over a few °C). This latter effect was attributed to n-clustering attractive interactions triggered at a critical surface density.

In the present work we report direct evidence of a vertical phase separation for a water soluble polymer brush. We used neutron reflectivity (NR) to study the conformational change of PNIPAM brushes grafted at high surface density from gold and silicon oxide surfaces by ATRP. For the brush on gold, the dry film thickness was 360 Å. The molecular weight and surface density were estimated to be 71 000 g/mol and 0.0054 chains/Å^2, respectively [24]. This sample will henceforth be referred to as 71G. The chains are strongly overlapping, with a reduced surface density of $\sigma\pi R_g^2 \sim 136$ at 20 °C. For the brush on silicon oxide, the dry film thickness was 570 Å. The molecular weight and surface density were estimated to be 209 000 g/mol and 0.0021 chains/Å^2, respectively. The chains are also strongly overlapping for this sample, with a reduced surface density of $\sigma\pi R_g^2 \sim 173$ at 20 °C. This sample will henceforth be referred to as 209S. For both of these samples, a nonmonotonic change in conformation with temperature was observed. We report the data below and discuss the results in the context of the first-order vertical phase separation for the PNIPAM system predicted by two state models for water-soluble polymer brushes.

The PNIPAM brushes were synthesized using ATRP, where an alkyl halide was employed as an initiator and a transition-metal complex as a catalyst to create a polymer radical. The detailed synthetic procedure for the sample grafted from gold is described elsewhere [22]. In order to prepare PNIPAM brushes directly on silicon oxide, an organosilane containing a bromo-isobutyrate ATRP initiator was used. The synthetic procedure for the organosilane initiator [11-(2-bromo-2-methylpropinonyloxy)undecyltrichlorosilane] is described in detail elsewhere [25]. The silicon wafers were cleaned with piranha solution, rinsed with water, and then dried in a stream of nitrogen. The cleaned wafers were placed in a toluene solution containing a mixture of undecyltrichlorosilane and initiator and the container was heated at 60 °C for 4 h. The silicon wafers were then removed, washed with toluene and ethanol, and then dried in a stream of nitrogen. The initiator-modified samples were placed into a water solution containing the NIPAM monomer and CuBr/N,N,N',N',N''—pentamethyldiethylenetriamine catalyst and allowed to react for various periods of time [26]. The reaction was carried out in a glove box purged with dry nitrogen. The samples were rinsed with THF to terminate the reaction and then cleaned with deionized water and methanol to remove unbound polymer.

The NR measurements were performed on the NG7 reflectometer at NIST. A fixed wavelength of 4.75Å was used. Reflectivity data from the protonated PNIPAM layers in deuterated water were obtained using a liquid cell over a range of temperature from 20 to 41 °C. Neutron reflectivity probes the scattering length density (SLD) profile normal to the surface, which is determined by the density and atomic composition. The SLD profiles were converted to volume fraction profiles assuming additivity of volumes. The SLD profiles were composed of a stack of slabs, where each slab was assigned an SLD, a thickness, and a roughness. The data were analyzed using a small number of unconstrained layers (one or two) to represent the grafted PNIPAM profile. To constrain the fits to the NR data, the thicknesses and SLD values of the Cr, Au, silicon oxide, SAM, and dry PNIPAM layers were determined in separate experiments and fixed in the analyses. The reflectivity was calculated from the stack of slabs using the optical matrix method [27]. Best-fit profiles were determined by minimization of least squares. X-ray reflectivity, which determines the electron density profile normal to the surface [28], was used to determine some of the layer thicknesses mentioned above and was performed both at Sandia National Labs and at NIST.

NR data for 71G in D_2O for a sequence of temperatures beginning at 20 °C, after increasing to 41 °C (well above the LCST), and then upon subsequent cooling are shown in Fig. 1(a). The data are displayed as reflectivity $\times q^4$ to compensate for the q^{-4} decay due to the Fresnel law. The data are shifted on the y-axis for clarity. Reflectivity curves were obtained for 1 °C increments in temperature (some data not shown). Large changes are observed as a function of temperature for $q < 0.04\text{Å}^{-1}$, reflecting the change in the PNIPAM segment concentration profile. The reflectivity for $q > 0.04\text{Å}^{-1}$ is mostly determined by the metal layers, and shows little change with temperature. The change in the reflectivity data with temperature is nonmonotonic, as shown in the expanded view of the lower q data in Fig. 1(b). The reflectivity returned to that of the original curve as the temperature was lowered back to 20 °C. Good reversibility was obtained for several heating-cooling cycles. An hysteresis was consistently observed in the heating and cooling cycle.

Best-fit profiles for selected temperatures are shown in Fig. 2. The profiles show that the PNIPAM chains expand significantly upon cooling from 41 to 20 °C. Specifically, the maximum extent of the layer, defined arbitrarily as the dis-

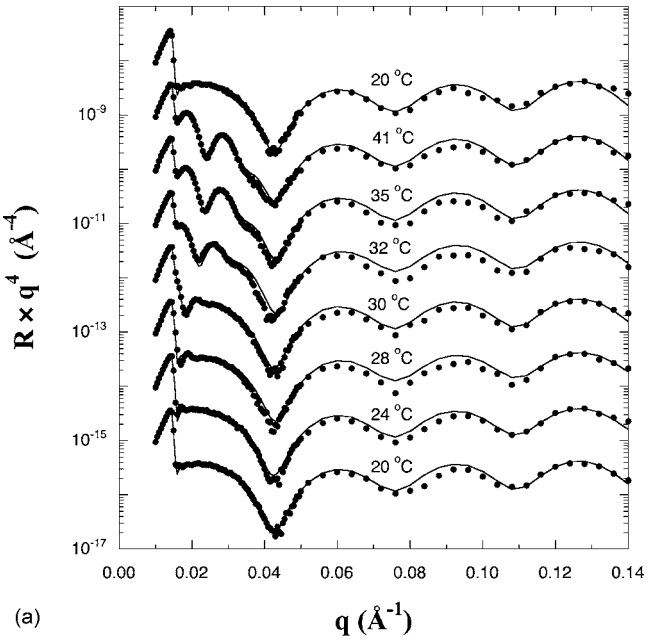

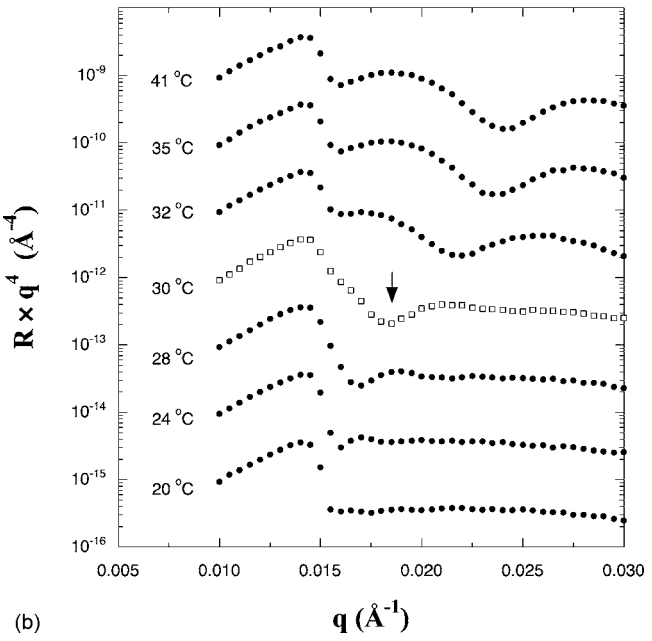

FIG. 1. (a) Neutron reflectivity data from 71G for a series of temperatures in D_2O. The curves through the data correspond to best-fits segment concentration profiles shown in Fig. 2. (b) Expanded view of the lower q region that shows the nonmnotonic change in the data with temperature.

tance at which the volume fraction drops to 0.02, increased from ~610Å to ~840Å over this temperature range. This has been discussed elsewhere [29]. The focus of this report is the nonmonotonic change in the shape of the profile in passing from 41 to 20 °C. At 41 °C, the profile is steplike with a smooth transition to bulk water. This indicates that the brush exists in a single dense phase. At 32 °C, the profile can still be described by a single layer, although the brush is less dense and more expanded relative to that at 41 °C. However, upon further decrease in temperature to 30 °C, a single layer profile is no longer an adequate description of the data. This

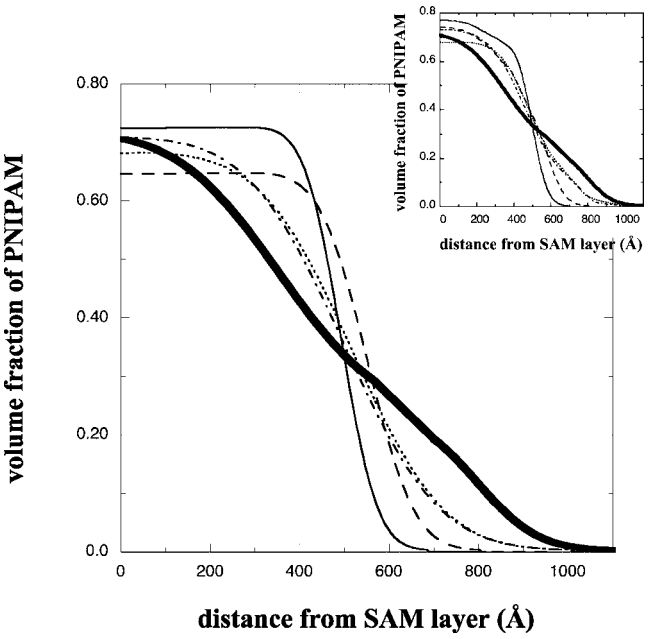

FIG. 2. Best-fit segment concentration profiles for 71G for 41 °C (—), 32 °C (— —), 30 °C (▬), 28 °C (– –), 20 °C (·–·–), in D_2O. The profile at 30 °C was obtained using a bilayer in the fitting analysis, whereas all other profiles were obtained using a single layer. The inset shows the best-fit concentration profiles using a bilayer function for all temperatures. The change in profile shape through the transition is still apparent.

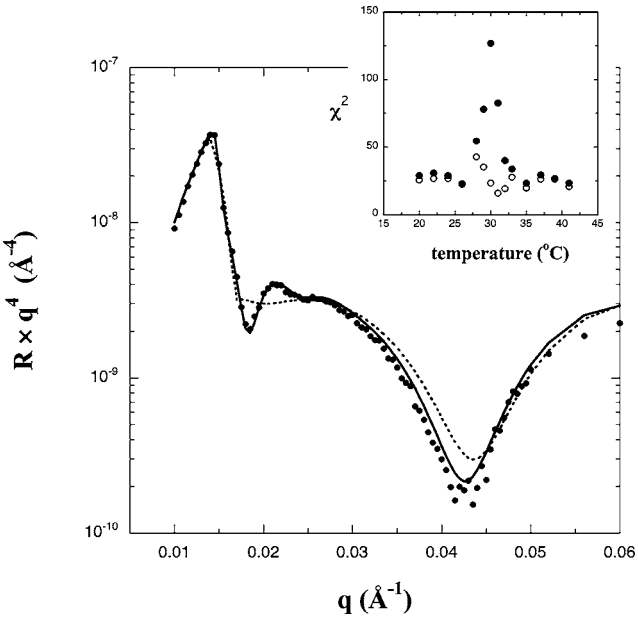

FIG. 3. Neutron reflectivity data from 71G at 30 °C in D_2O. The data are compared with the best-fit curves using a single layer profile (···) and a bilayer profile (—). The inset shows the χ^2 values for all temperatures using both single layer (●) and bilayer (◯) functions in the fitting. For a single layer function, a large increase in χ^2 occurs for the narrow range of temperatures from 31 to 29 °C. The improvement with a bilayer is only significant for that same temperature range.

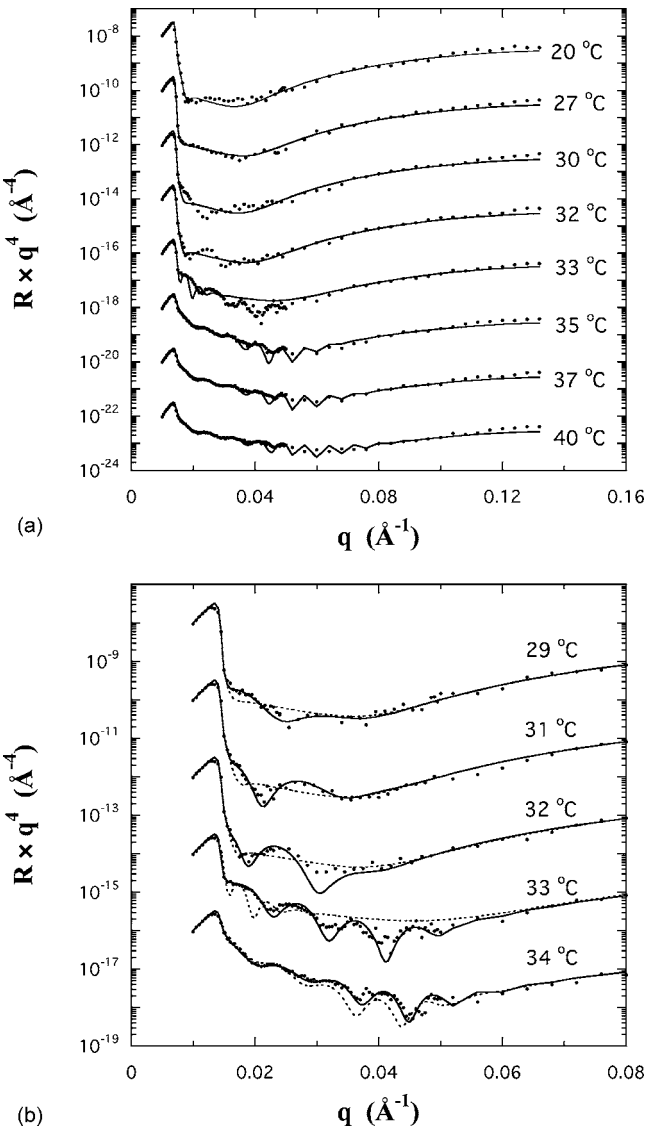

FIG. 4. (a) Neutron reflectivity data from 209S for a series of temperatures in D_2O. The curves through the data correspond to best-fits using a single layer to describe the PNIPAM brush. (b) Expanded view of the lower q region for temperatures in the transition region. Solid lines correspond to fits using two layers to describe the PNIPAM brush, and dashed lines indicate fits using one layer to describe the PNIPAM brush.

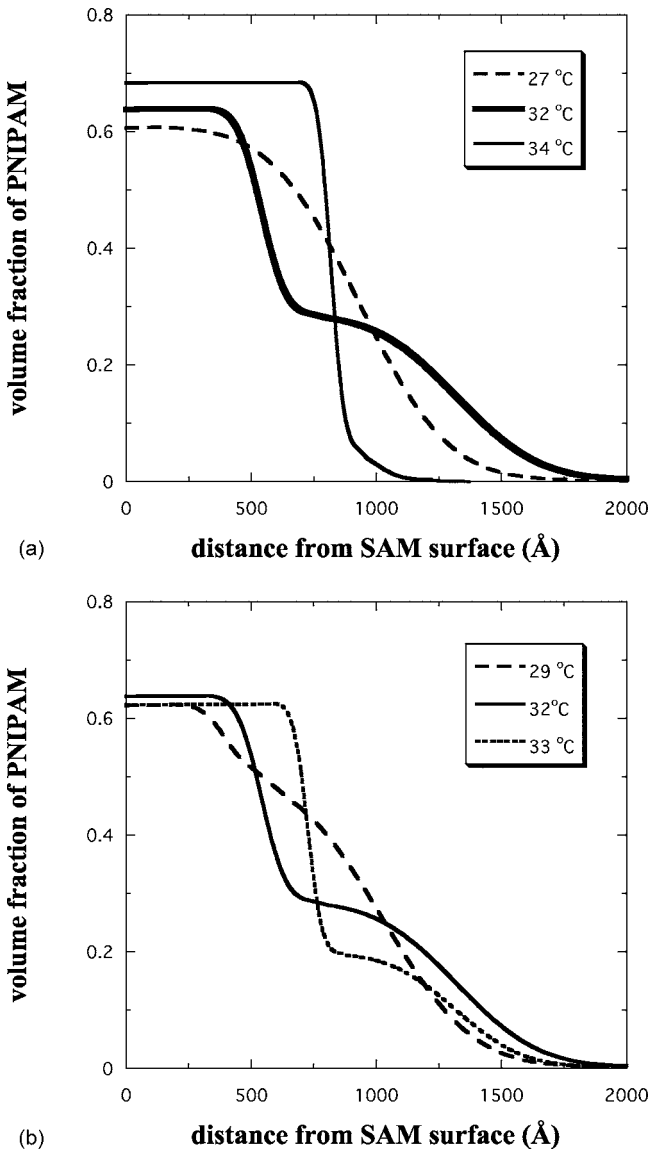

FIG. 5. (a) Best-fit segment concentration profiles for 209S at 27, 32, and 34 °C showing the dramatic change in profile shape in the transition region. (b) Best-fit segment concentration profiles for 209S at 31, 32, and 33 °C showing the gradual change in the shape of the bilayer profile through the transition.

is shown in detail in Fig. 3. Agreement with the data requires a bilayer profile in which the segment concentration in the tail and at the surface is increased at the expense of the segment concentration in the middle of the profile. A similar profile shape also results at 31 °C and at 29 °C. At 28 °C the data are again consistent with a single layer profile, and that continues to be the case upon further cooling to 20 °C. The inset to Fig. 3 shows that the χ^2 values obtained using a single layer increase substantially for a narrow range of temperatures near the LSCT (31–29 °C), and that the improvement with a bilayer is only significant for this transition region. This clearly demonstrates a significant change in profile shape near the transition. The inset to Fig. 2 shows that the conclusion of a nonmonotonic change in profile shape still results if a bilayer function is used in the fitting for all temperatures. In that case, the fits converge to a profile shape that approximates a single layer for temperatures far from the transition.

Analogous results for 209S are shown in Figs. 4 and 5. Figure 4(a) shows the reflectivity for a series of temperatures beginning at 20 °C and then increasing to 40 °C. The solid lines are best fits using a single layer to describe the PNIPAM brush. The fits are adequate from 20 to 27 °C and for 35 to 40 °C, but are clearly inadequate for 30 to 33 °C. Figure 4(b) shows an expanded view of the data for 29 to 34 °C, comparing best-fits using both single layer and bilayer functions for the PNIPAM brush. In the transition region where the single layer is inadequate, the bilayer function is an adequate description of the data. The profiles for 27, 32,

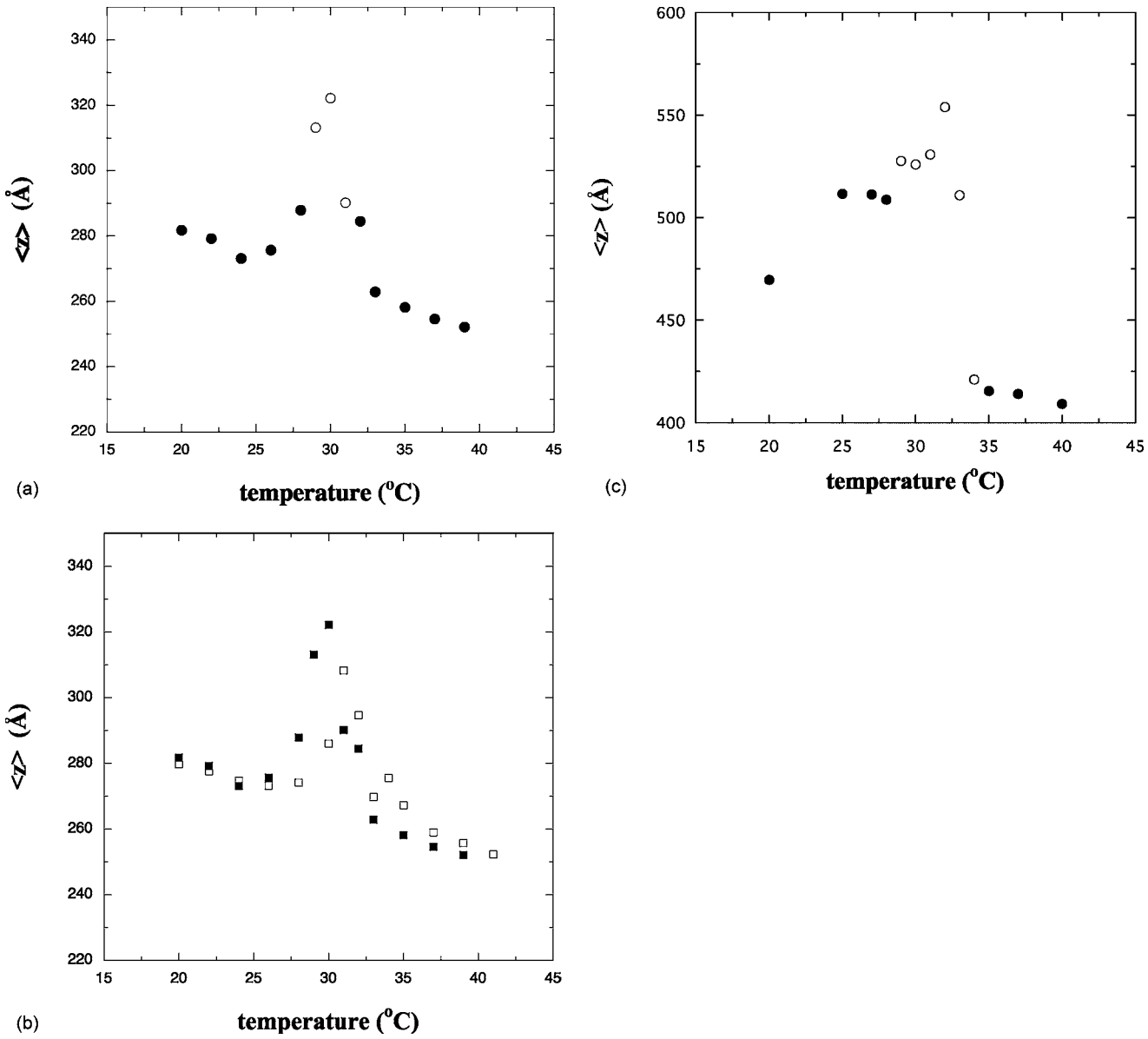

FIG. 6. (a) First moment of the segment volume fraction profiles for 71G as a function of temperature upon cooling from 41 °C. The symbols indicate results using bilayer (◯) and single layer (●) functions in the fits. (b) Comparison of the change in first moment for heating (□) versus cooling (■) 71G through the transition. The maximum occurs at a slightly higher temperature when heating through the transition. (c) First moment of the segment volume fraction profiles for 209S as a function of temperature upon heating from 20 °C. The symbols indicate results using bilayer (◯) and single layer (●) functions in the fits.

and 34 °C are compared in Fig. 5(a). The strong change in the profile shape at the transition is even more apparent for this sample than for 71 G. Profiles for several temperatures in the transition region are plotted in Fig. 5(b). This shows the progressive change in profile shape. A slight excess of segment density appears first in the central portion of the profile. Upon further heating, the transition between the two layers becomes sharper and the segment density in the layer furthest from the substrate decreases.

Whereas the trend from a single layer to a bilayer and back to a single layer form is consistent with the predictions of Baulin and Halperin, an important aspect of our data is not captured in their predictions. For the temperature range where the bilayer profile is observed, the extension of the profile into D_2O is significantly greater than that at temperatures on either side of that range. This is shown in Fig. 6(a) for 71G, where the first moment of the segment profile is plotted versus temperature. A peak in this plot results even when a single layer function is fit to the data at all temperatures, which demonstrates that the peak is not an artifact of using a bilayer function near the transition. The peak results for both heating and cooling through the transition as shown in Fig. 6(b), but is shifted to slightly higher temperatures for the case of heating through the transition. Analogous results for 209S are shown in Fig. 6(c), which also displays a peak in the first moment of the profile through the transition. We do not fully understand this effect. It might be due to an increased local stiffness resulting from changes in the local

interactions near the transition, such as ordering of water molecules around the chain segments. Alternatively, it might reflect nonuniform swelling of the brush, and the interplay of the temperature and segment volume fraction dependencies. For example, if, rather than a uniform swelling of the brush, a dilute tail emerges first from the contracted layer upon cooling, the low concentration in the tail will result in a low value of χ_{eff} and relatively good solvent conditions. If subsequent swelling upon further cooling occurs by an increase in the segment density in the tail, the increased segment density will initially cause stronger swelling due to the osmotic interaction. Eventually however, the concentration dependence of χ_{eff} will take over and the decreasing solvent quality due to the increased segment density in the tail will cause the extension of the tail to decrease. Thus, it appears that nonuniform swelling could cause the overall extension of the chains and the first moment of the profile to pass through a maximum. The present observation appears to be similar in nature to the maximum in ΔR_h as a function of temperature reported by Hu and Wu for PEO chains grafted to PNIPAM microgels [23].

We also considered the possibility that lateral effects might play a role. Lateral aggregation within polymer brushes was reported by Lai and Binder using a Monte Carlo simulation [30]. Balaz and co-workers [31,32] later studied lateral instabilities in grafted layers in a poor solvent (UCST system) using a two-dimensional numerical SCF theory. However, atomic force microscopy images of our PNIPAM films in water at 20 and 40 °C showed very little change in lateral aggregation.

NR data have also been obtained for two lower molecular weight samples grafted at the same high surface density (identical SAM composition) as 71G. These samples had molecular weights of 44 000 and 13 000 g/mol. The change in profile shape through the transition described above becomes less signficant with decreasing N. A smaller, but still measurable, effect in the profile shape and in the first moment were observed for the 44 000 g/mol sample [33], but no such effects were apparent for the 13 000 g/mol sample. The effect of molecular weight on vertical phase separation within a brush has not yet been studied theoretically. We also note that no such nonmonotonic change in profile shape was observed for a brush grafted from gold with a relatively high molecular weight of 152 000 g/mol but with a lower surface density of $\sigma=6.3\times10^{-4}$ Å^{-2} [34]. Thus the effect is most prominent for brushes with both high surface density and high molecular weight. The former is consistent with the prediction of Baulin and Halperin of a critical surface density for vertical phase separation.

In conclusion, we report direct evidence for a vertical phase separation in water-soluble polymer brushes using NR. PNIPAM chains were grafted at high density on both gold and silicon oxide using ATRP. Upon heating or cooling through the transition, the segment concentration profile changed from a single layer, to a distinct bilayer, and then back to a single layer. The bilayer profile was observed for a narrow temperature range near the LCST and corresponded to a sharp increase in the first moment of the profile. The effect became weaker with decreasing molecular weight or surface density.

We would like to thank Avi Halperin for helpful discussions. Sandia is a multiprogram laboratory operated by Sandia Corporation, a Lockheed Martin Company, for the United States Department of Energy under Contract No. DE-AC04-94AL85000. We acknowledge the support of the National Institute of Standards and Technology, U.S. Department of Commerce, in providing the neutron research facilities used in this work, and also support from the Office of Naval Research.

[1] *Poly(ethylene glycol) Chemistry*, edited by J. M. Harris (Plenum Press, New York, 1992).
[2] P. S. Stayton, T. Shimoboji, C. Long, A. Chilkoti, G. Chen, J. M. Harris, and A. S. Hoffman, Nature (London) **378**, 472 (1995).
[3] Y. S. Park, Y. Ito, and Y. Imanishi, Langmuir **14**, 910 (1998).
[4] J. Zheng, S. R. Northrup, and P. J. Hornsby, In Vitro Cell. Dev. Biol.: Anim. **34**, 679 (1998).
[5] L. K. Ista, V. H. Perez-Luna, and G. P. Lopez, Appl. Environ. Microbiol. **65**, 2552 (1999).
[6] A. Matsuyama and F. Tanaka, Phys. Rev. Lett. **65**, 341 (1990).
[7] S. Bekiranov, R. Bruinsma, and P. Pincus, Phys. Rev. E **55**, 577 (1997).
[8] E. Dormidontova, Macromolecules **35**, 987 (2002).
[9] G. Karlstrom, J. Phys. Chem. **89**, 4962 (1985).
[10] P.-G. de Gennes, CR Acad, Sci. II (Paris) **117**, 313 (1991).
[11] S.-Y. Lin, K.-S. Chen, and L.-R. Chu, Polymer **40**, 2619 (1999).
[12] Y. Katsumoto, T. Tanaka, H. Sato, and Y. Ozaki, J. Phys. Chem. A **106**, 3429 (2002).
[13] H. G. Schild, Prog. Polym. Sci. **17**, 163 (1992).
[14] K. Kubota, S. Fujishige, and I. Ando, J. Phys. Chem. **94**, 5154 (1990).
[15] M. Wagner, F. Brochard-Wyart, H. Hervet, and P.-G. de Gennes, Colloid Polym. Sci. **271**, 621 (1993).
[16] W. L. Mattice, S. Misra, and D. H. Napper, Europhys. Lett. **28**, 603 (1994).
[17] V. A. Baulin and A. Halperin, Macromol. Theory Simul. **12**, 549 (2003).
[18] V. A. Baulin, E. B. Zhuina, and A. Halperin, J. Chem. Phys. **119**, 10977 (2003).
[19] F. Afroze, E. Nies, and H. Berghmans, J. Mol. Struct. **554**, 55 (2000).
[20] P. W. Zhu and D. H. Napper, J. Colloid Interface Sci. **164**, 489 (1994).
[21] P. W. Zhu and D. H. Napper, Colloids Surf., A **113**, 145 (1996).
[22] S. Balamurugan, S. Mendez, S. S. Balamurugan, M. J. O'Brien II, and G. P. Lopez, Langmuir **19**, 2545 (2003).
[23] T. Hu and C. Wu, Phys. Rev. Lett. **83**, 4105 (1999).
[24] A PNIPAM sample was polymerized in solution simultaneous with a surface polymerization on a substrate with a SAM con-

taining 90% OH termination, as for the present sample. Gel permeation chromatograhy (GPC) analysis of this sample using polystyrene standards for calibration gave a weight average molecular weight of 98 500 g/mol and a polydispersity of 2.1. The surface polymerization yielded a dry film thickness of 500 Å+/−20 Å. The weight average molecular weight from GPC for the bulk polymerization and the dry film thickness of the surface polymerization correspond to a surface density of 5.4×10^{-3}chains/Å^2. Assuming the surface density is constant for all polymerizations with 90% OH termination, this value combined with the dry film thickness of 360 Å for the present sample corresponds to a weight average molecular weight of 71 000 g/mol. In Refs. [29,33], we reported a surface density of 3.1×10^{-3}chains/Å^2 for 71G. This value was obtained assuming that the melt density of PNIPAM is 1.0 g/cm^3. However, the density obtained from the measured SLD of the dry sample is 1.76 g/cm^3, which corresponds to the value 5.4×10^{-3}chains/Å^2 reported above.

[25] K. Matyjaszewski, P. J. Miller, N. Shukla, B. Immaraporn, A. Gelman, B. B. LuoKala, T. M. Siclovan, G. Kickelbick, T. Vallant, H. Hoffmann, and T. Pakula, Macromolecules **32**, 8716 (1999).

[26] M. Kaholek, W.-K. Lee, S.-J. Ahn, H. Ma, K. C. Caster, B. LaMattina, and S. Zauscher, Chem. Mater. **16**, 3688 (2004).

[27] D. Styrkas, S. J. Doran, V. Gilchrist, J. L. Keddie, J. R. Lu, E. Murphy, R. Sackin, T.-J. Su, and A. Tzitzinou, *Polymer Surfaces and Interfaces III*, edited by R. W. Richards and S. K. Peace (John Wiley & Sons Ltd., New York, 1999).

[28] T. P. Russell, Mater. Sci. Rep. **5**,171 (1990).

[29] H. Yim, M. S. Kent, S. Satija, S. Mendez, S. S. Balamurugan, S. Balamurugan, and G. P. Lopez, J. Polym. Sci., Part B: Polym. Phys. **42**, 3302 (2004).

[30] P. Y. Lai and K. J. Binder, J. Chem. Phys. **96**, 586 (1992).

[31] C. Yeung, A. C. Balaz, and D. Jasnow, Macromolecules **26**, 1914 (1993).

[32] K. Huang and A. C. Balaz, Macromolecules **26**, 4736 (1993).

[33] H. Yim, M. S. Kent, S. Mendez, S. S. Balamurugan, S. Balamurugan, G. P. Lopez, and S. Satija, Macromolecules **37**, 1994 (2004).

[34] H. Yim, M. S. Kent, S. Mendez, G. P. Lopez, S. Satija, and Y. Seo (submitted).